Upper limit for the branching ratio of $K_S \rightarrow e^+e^-$decay

The CPLEAR Collaboration

R. Adler[2], T. Alhalel[11], A. Angelopoulos[1], A. Apostolakis[1], E. Aslanides[11], G. Backenstoss[2], P. Bargassa[13], C.P. Bee[9], O. Behnke [17], A. Benelli [9], V. Bertin[11], F. Blanc[7,13], P. Bloch[4], P. Carlson[15], M. Carroll[9], J. Carvalho[5], E. Cawley[9], S. Charalambous[16], G. Chardin[14], M.B. Chertok[3], A. Cody[9], M. Danielsson[15], M. Dejardin[14], J. Derre[14], A. Ealet[11], B. Eckart[2], C. Eleftheriadis[16], I. Evangelou[8], L. Faravel [7], P. Fassnacht[11], C. Felder[2], R. Ferreira-Marques[5], W. Fetscher[17], M. Fidecaro[4], A. Filipčič[10], D. Francis[3], J. Fry[9], E. Gabathuler[9], R. Gamet[9], D. Garreta[14], H.- J. Gerber[17], A. Go[3,15], C. Guyot[14], A. Haselden[9], P.J. Hayman[9], F. Henry-Couannier[11], R.W. Hollander[6], E. Hubert[11], K. Jon-And[15], P.-R. Kettle[13], C. Kochowski[14], P. Kokkas[2], R. Kreuger[6,13], R. Le Gac[11], F. Leimgruber[2], A. Liolios[16], E. Machado[5], I. Mandić[10], N. Manthos[8], G. Marel[14], M. Mikuž[10], J. Miller[3], F. Montanet[11], T. Nakada[13], B. Pagels [17], I. Papadopoulos[16], P. Pavlopoulos[2], J. Pinto da Cunha[5], A. Policarpo[5], G. Polivka[2], R. Rickenbach[2], B.L. Roberts[3], T. Ruf[4], L. Sakeliou[1], P. Sanders[9], C. Santoni[2], M. Schäfer[17], L.A. Schaller[7], T. Schietinger[2], A. Schopper[4], P. Schune[14], A. Soares[14], L. Tauscher[2], C. Thibault[12], F. Touchard[11], C. Touramanis[4], F. Triantis[8], E. Van Beveren[5], C.W.E. Van Eijk[6], S. Vlachos[2], P. Weber[17], O. Wigger[13], M. Wolter[17], C. Yeche[14], D. Zavrtanik[10] and D. Zimmerman[3]

presented by I. Mandić

[1]University of Athens, [2]University of Basle, [3]Boston University, [4]CERN, [5]LIP and University of Coimbra, [6]Delft University of Technology, [7]University of Fribourg, [8]University of Ioannina, [9]University of Liverpool, [10]J. Stefan Inst. and Phys. Dep., University of Ljubljana, [11]CPPM, IN2P3-CNRS et Université d'Aix-Marseille II, [12]CSNSM, IN2P3-CNRS, Orsay, [13]Paul-Scherrer-Institut(PSI), [14]CEA, DSM/DAPNIA CE-Saclay, [15]KTH-Stockholm, [16]University of Thessaloniki, [17]ETH-IPP Zürich

A measurement of the branching ratio for $K_S \rightarrow e^+e^-$ decay was performed with the CPLEAR detector at LEAR. Full event reconstruction together with calorimeter e/π separation allowed for powerful background rejection and high signal acceptance. Analysis of data taken up to 1994 yields the result: $Br(K_S \rightarrow e^+e^-) < 4.2 \cdot 10^{-7}$ (90 % CL).

1. INTRODUCTION

The decay $K_S \rightarrow e^+e^-$ is not allowed in the first order of the weak interaction but it can proceed through higher orders. In the frame of the Standard Model the branching ratio is expected to be small : the $Br(K_L \rightarrow e^+e^-)$ was measured to be $< 4.1 \times 10^{-11}$ (90% CL) [1] and the $Br(K_S \rightarrow e^+e^-)$ is expected to be further suppressed by two orders of magnitude due to the shorter lifetime. A significantly higher value than expected would point to new physics.

The current experimental value of the branching ratio is $Br(K_S \rightarrow e^+e^-) < 2.8 \times 10^{-6}$ (90% CL) [2]. Here we report about a new measurement of this branching ratio with the CPLEAR detector at LEAR.

2. CPLEAR EXPERIMENT

The CPLEAR experiment was designed to study CP violation in the neutral kaon system using strangeness tagged K^0s and $\bar{K}^0$s and it accumulated a large number of events. The data can be used for the search of rare K_S-decay since most of the neutral kaons decay as K_S in the detector while the long-lived component escapes.

Neutral kaons are produced in $p\bar{p}$ annihilations,

$$p\bar{p} \rightarrow K^- \pi^+ K^0 \quad \text{or} \quad K^+ \pi^- \bar{K}^0 \tag{1}$$

with a branching ratio of 0.2% per channel. Antiprotons with a momentum of 200 MeV/c are supplied by LEAR at a rate of 1 MHz. They annihilate with protons in a hydrogen gas target at 16 bar, in the center of the detector. The detector is placed in a solenoid providing an uniform magnetic field of 0.44 T. Annihilation products are detected with ten tracking-chamber layers consisting of multiwire proportional chambers, drift chambers and streamer tubes. Particle identification, in particular charged-kaon identification is performed by a 32-sector scintillator-Čerenkov-scintillator detector allowing pulse-height and time-of-flight measurements. Electron and photon showers are sampled by a 18-layer electromagnetic calorimeter with lead converters and high-gain tubes. A fast dedicated hardwired trigger system is tuned to efficient selection of the annihilation channels (1) at the highest possible rate. A detailed description of the detector can be found in Ref. [3].

3. NORMALIZATION

The number of K_S - required to calculate the branching ratio - is obtained by counting $K_S \rightarrow \pi^+\pi^-$ decays in the same data sample as used for the $K_S \rightarrow e^+e^-$ search. This number, together with known branching ratios of K^0 decays, is also used to normalize Monte Carlo (MC) data in order to obtain the level of expected background.

$K_S \rightarrow \pi^+\pi^-$ decays are selected as reported in [4] and only the events where the K_S decay-time is between 1 and 2 τ_S are counted. The background in this kind of selection is negligible [4].

In the data used for this analysis (up to 1994 included) the total number of $K_S \rightarrow \pi^+\pi^-$ decays in the normalization sample is $\approx 2 \times 10^7$.

4. EVENT SELECTION

At the initial stage of the analysis most of the background consists of $K_S \rightarrow \pi^+\pi^-$ decays. The expected background is determined from a MC

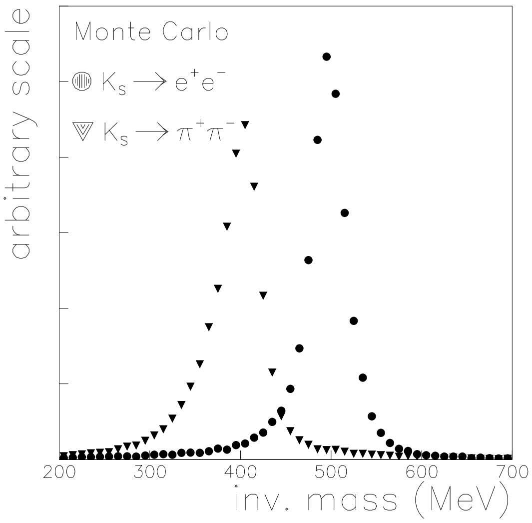

Figure 1. Distribution of e^+e^- invariant mass for signal and background events.

simulation of K^0 decays ($\bar{p}p \rightarrow K^\pm\pi^\mp K^0; K^0 \rightarrow$ two charged particles), using the normalization described above. The rejection of the background is done by using kinematical methods and electron identification with the calorimeter.

4.1. Kinematical selection

Events with four tracks and zero total charge are selected. A good reconstruction quality is required for all tracks. The annihilation (primary) and the decay (secondary) vertex must be well reconstructed. There must be at least one charged kaon candidate and the probability of the kinematical fit requiring the K^0 missing mass at the primary vertex must be $> 10\%$ to improve the selection of the annihilation channel $K^\pm\pi^\mp K^0$. Events from other annihilation channels - without a K^0 in the final state - are further reduced by requiring that neither four nor three tracks can be attached to a single vertex.

The opening angle of the secondary tracks has to be larger than 11^o in order to remove e^+e^- pairs from γ conversions or π^0 Dalitz decays.

At this stage the acceptances for both the signal ($K_S \rightarrow e^+e^-$) and the main background

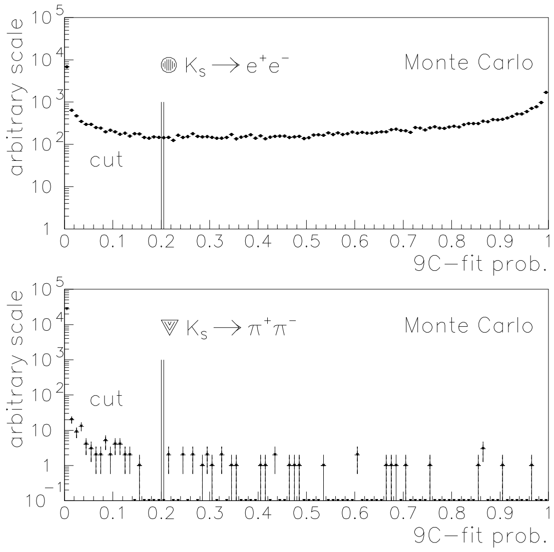

Figure 2. Distribution of 9C-fit probability for signal and background.

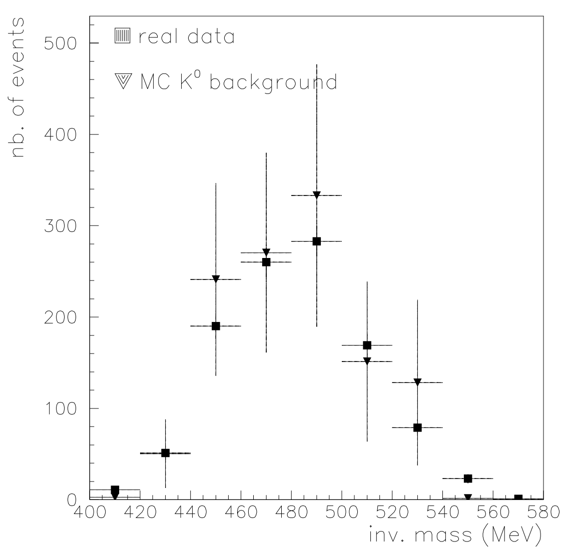

Figure 3. e^+e^- invariant mass distribution after kinematical selection.

($K_S \rightarrow \pi^+\pi^-$) are of the same magnitude. The separation between these two decays relies on the invariant mass of the secondary particles, as shown on Fig. 1 .

An optimal separation can be obtained by performing a kinematical and geometrical fit to the $\bar{p}p \rightarrow K^\pm\pi^\mp K^0(K^0 \rightarrow e^+e^-)$ hypothesis with nine constraints. The constraints require conservation of energy and momentum, the missing mass at the annihilation vertex to be equal to K^0 mass, the intersections of two track helices at the annihilation and decay vertex, respectively, and the K^0 momentum to be collinear with the line joining the two vertices. The distribution of the constraint fit probability can be seen in Fig. 2.

Requiring a 9C-fit probability > 0.2, together with all the previous mentioned cuts, reduces by a factor 10^3 the $K_S \rightarrow \pi^+\pi^-$ background at the cost of 65% of the signal.

The MC simulation shows that a large fraction of the remaining background consists of events where the primary pion is exchanged with the secondary pion having a charge opposite to the kaon. Such events can be recognised because the invariant mass of the pion taken as a primary and the opposite charge secondary pion clusters at the K^0 mass. Performing a 1C-fit, requiring this invariant mass to be equal to K^0 mass with a probability $< 10\%$, the efficiency for $K_S \rightarrow \pi^+\pi^-$ events is reduced by another factor of 10 loosing 5% on signal acceptance.

The e^+e^- invariant mass distribution and the momentum distribution of the secondary tracks after kinematical selection are shown in Fig. 3 and Fig. 4, respectively, both for real and MC data. There is a good agreement between real and simulation data.

At this level the semileptonic decays ($K^0 \rightarrow \pi e\nu$) are no longer negligible because they represent 10% of the expected background.

4.2. Calorimeter electron identification

The calorimeter electron identification provides a further reduction of the background.

The CPLEAR electromagnetic calorimeter is an 18-layer high-granularity sampling calorimeter. It consists of high-gain tubes of 4×4.5

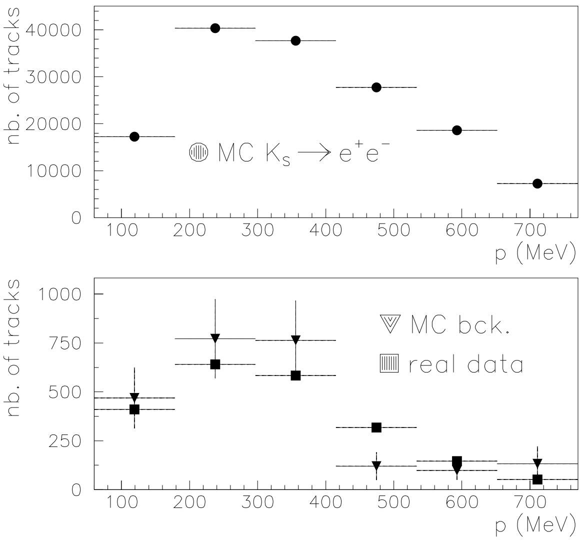

Figure 4. Momentum distribution of secondary tracks for MC signal, real data, and MC expected background.

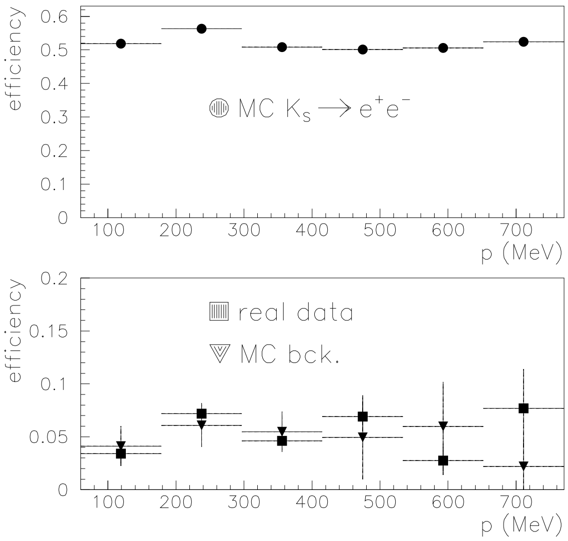

Figure 5. Efficiency of electron identification at 4% allowed pion contamination for MC signal, real data and MC expected background.

mm^2 cross-section in active layers interleaved with $1/3X_0$ Pb plates. Because of the high granularity, e/π separation can be performed by exploiting shower topologies.

Among the components of the CPLEAR detector which could be used for particle identification, the calorimeter is the most suitable for this measurement, because of the high momentum range of electrons from $K_S \rightarrow e^+e^-$ decays, (see Figs. 4 and 5).

The full power of calorimeter identification is obtained by requiring both secondary tracks to be recognized as electrons i.e. both tracks must have a low pion-probability in the calorimeter. Fig. 6-up gives for the real data and the expected background the number of events that survive the kinematical selection and the electron identification, as a function of the pion-probability cut used for e/π separation. In Fig. 6-down the efficiency of the electron identification for MC signal events is also shown. Finally the cut chosen corresponds to a 4% probability for a pion to fake an electron.

After the electron identification the background consists of 80% of semileptonic ($K^0 \rightarrow \pi e\nu$) events.

5. Upper limit

We would like to stress that all the cuts mentioned in Section 4 were chosen so to get the best statistical significance of a potential signal. The ratio $\eta_{ee}/\sqrt{\eta_b}$ - where η_{ee} and η_b are signal and background acceptances respectively - was maximised by changing in steps the cuts in MC data.

Zero events are found after applying these cuts on real data. The number of expected background events is 2.6 ± 0.7.

The upper limit of the number of signal events for a Poisson process including a background is calculated using the following equation [1]:

$$1 - \epsilon = 1 - \frac{e^{-(\mu_b+\mu_s)} \sum_0^{n_0} \frac{(\mu_b+\mu_s)^n}{n!}}{e^{-\mu_b} \sum_0^{n_0} \frac{\mu_b^n}{n!}} \tag{2}$$

where $1-\epsilon$ is the confidence level, μ_b is the expected number of background events (from MC), μ_s is the number of signal events and n_0 is the number of observed events.

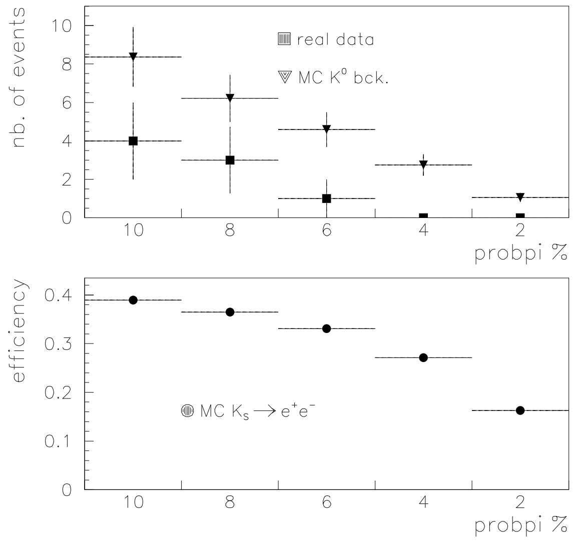

Figure 6. Number of real and MC expected background events (up) and efficiency of MC signal events (down) as a function of pion probability in the calorimeter required for both secondary tracks.

With zero observed events and 2.6 expected background events the upper limit at 90% CL for the number of signal events is $\mu_s = 2.4$. Using this number the branching ratio can be expressed from:

$$\mu_s = \frac{\eta^{ee}}{\eta^n}\frac{N^n_{2\pi}}{\mathrm{Br}(2\pi)} \cdot \mathrm{Br(ee)} \tag{3}$$

where η^{ee} is the signal acceptance, η^n is the acceptance for $\mathrm{K_S} \to \pi^+\pi^-$ events used for normalization and $N^n_{2\pi}$ is the number of these events, $\mathrm{Br}(2\pi)$ and Br(ee) are the branching ratios. The relative acceptance η^{ee}/η^n is $\approx 18\%$. Using the data collected from 1992 to 1994, we obtain

$$\frac{\eta^{ee}}{\eta^n}\frac{N^n_{2\pi}}{\mathrm{Br}(2\pi)} = 5.68 \cdot 10^6 \tag{4}$$

thus setting the upper limit of the branching ratio of $\mathrm{K_S} \to \mathrm{e^+e^-}$ decay:
$\mathrm{Br(K_S} \to \mathrm{e^+e^-}) < 4.2 \times 10^{-7}$ with 90% CL

6. PERSPECTIVES

In 1995 the CPLEAR detector was upgraded. A new proportional chamber was installed at 1.7 cm radius which resulted in an improved pionic background rejection by the trigger. The number of $\mathrm{K_S}$ decays collected in 1995 is approximately equal to the statistics of all previous years of running.

In addition a dedicated first level filtering of data for the $\mathrm{K_S} \to \mathrm{e^+e^-}$ channel resulted in three times higher signal acceptance.

A preliminary analysis of 1/3 of 1995 data showed that with the same cuts, as described above, an upper limit Br(ee)$< 5 \times 10^{-7}$ at 90% CL could be obtained.

From this it was estimated that with the full statistics CPLEAR should be able to set an upper limit of 1×10^{-7}.

REFERENCES

1. Review of Particle Properties, *Phys. Rev.* **D54** (1996) 166.
2. A. M. Blick et. al., *Phys. Lett.* **B334** (1994) 234.
3. R. Adler et al.,*Nucl. Instr. and Meth.* **A379** (1996) 76.
4. R. Adler et al., *Phys. Lett.* **B363** (1995) 243.